Molecular Biology of the Cell
Vol. 16, 3314–3322, July 2005

Synaptic Clusters of MHC Class II Molecules Induced on DCs by Adhesion Molecule–mediated Initial T-Cell Scanning[V]

Hortensia de la Fuente,*† María Mittelbrunn,*† Lorena Sánchez-Martín,‡ Miguel Vicente-Manzanares,* Amalia Lamana,* Ruggero Pardi,§ Carlos Cabañas,‡ and Francisco Sánchez-Madrid*

*Servicio de Inmunología, Hospital de la Princesa, Universidad Autónoma de Madrid, 28006 Madrid, Spain; ‡Instituto de Farmacología y Toxicología, CSIC-UCM, Facultad de Medicina, Universidad Complutense, 28040 Madrid, Spain; and §Vita-Salute San Raffaele University School of Medicine, 20132 Milano, Italy

Submitted January 4, 2005; Revised March 29, 2005; Accepted April 22, 2005
Monitoring Editor: Mark Ginsberg

Initial adhesive contacts between T lymphocytes and dendritic cells (DCs) facilitate recognition of peptide-MHC complexes by the TCR. In this report, we studied the dynamic behavior of adhesion and Ag receptors on DCs during initial contacts with T-cells. Adhesion molecules LFA-1- and ICAM-1,3-GFP as well as MHC class II-GFP molecules were very rapidly concentrated at the DC contact area. Binding of ICAM-3, and ICAM-1 to a lesser extent, to LFA-1 expressed by mature but not immature DC, induced MHC-II clustering into the immune synapse. Also, ICAM-3 binding to DC induced the activation of the Vav1-Rac1 axis, a regulatory pathway involved in actin cytoskeleton reorganization, which was essential for MHC-II clustering on DCs. Our results support a model in which ICAM-mediated MHC-II clustering on DC constitutes a priming mechanism to enhance antigen presentation to T-cells.

INTRODUCTION

Bone marrow–derived dendritic cells (DCs) are the most efficient Ag-presenting cells (APC), capturing and processing Ags and migrating to the paracortical region of lymph nodes, where they interact with naïve T-cells (Banchereau and Steinman, 1998). The interaction of T lymphocytes with APC involves different and sequential cellular events. Initially, the T-cell adheres transiently to the APC, scanning its surface for the presence of specific peptide-MHC complexes, which is independent of Ag recognition. This creates an initial contact interface that evolves into an Ag-dependent interaction and is accompanied by the reorganization of different molecules at T-cell-APC interface (Grakoui *et al.,* 1999; Montoya *et al.,* 2002b). Ag, adhesion, and costimulatory receptors as well as signaling intermediates are organized in supramolecular activation clusters (SMACs), comprising a central SMAC involved in Ag-dependent responses, in which the TCR, CD28, CD3, CD2, protein kinase C-θ, Lck, and Fyn molecules have been located surrounded by a peripheral SMAC containing adhesion-related components, such as the LFA-1 integrin and talin (Monks *et al.,* 1998; Grakoui *et al.,* 1999).

Initial T-cell-DC adhesion-mediated scanning facilitates recognition of Ag-MHC complexes by the TCR. Several pairs of adhesion molecules are involved in the initial adhesive interactions such as CD2/LFA-3, LFA-1/ICAM-1,-3, or ICAM-3/DC-SIGN. LFA-1 ligands include ICAM-1,-2,-3, and JAM-1 (Montoya *et al.,* 2002b; Ostermann *et al.,* 2002). ICAM-1 and ICAM-3 provide costimulatory signals to T lymphocytes (Van Seventer *et al.,* 1990; Campanero *et al.,* 1993; Juan *et al.,* 1994), and both have been localized at the T-cell-APC interface (Grakoui *et al.,* 1999; Montoya *et al.,* 2002a). Although LFA-1 binds to ICAM-3 with low affinity compared with ICAM-1 (Bleijs *et al.,* 2000), blocking antibodies directed against ICAM-3 have been shown to inhibit T-cell proliferation in DC-stimulated mixed leukocyte reactions (Starling *et al.,* 1995). These facts together with the high expression of ICAM-3 on naïve T lymphocytes support its role in initial transient contacts between T lymphocytes and APC (Montoya *et al.,* 2002a).

Although DCs are the most important APC, relatively little is known on the nature of the immune synapse (IS) formed between T-cells and DCs. An active role of DC actin cytoskeleton during IS formation has been reported (Al-Alwan *et al.,* 2003). The relative density of a given MHC-peptide complex on DC surface is quite low. Thus, cooperative mechanisms to enhance Ag presentation based on changes of surface density of MHC-II molecules may exist (Banchereau and Steinman, 1998).

We describe herein the organization and dynamics of adhesion and MHC class II molecules at the initial steps

This article was published online ahead of print in *MBC in Press* (http://www.molbiolcell.org/cgi/doi/10.1091/mbc.E05–01–0005) on May 4, 2005.

[V] The online version of this article contains supplemental material at *MBC Online* (http://www.molbiolcell.org).

† These authors contributed equally to this work.

Address correspondence to: Francisco Sánchez-Madrid (fsanchez.hlpr@salud.madrid.org).

Abbreviations used: Ag, antigen; APC, Ag presenting cell; c-SMAC, central supramolecular activation complex; DC(s), dendritic cell(s); DIC, differential interference contrast; Gp, glycophorin; IS, immune synapse; p-SMAC, peripheral supramolecular activation complex; SEB, staphylococcal enterotoxin B.

of DC interaction with T lymphocytes, as well as the role of ICAMs on the induction of MHC-II clustering at the DC- T lymphocyte contact area. Such clustering is induced by triggering of the LFA-1 integrin on mature DC and requires signaling involved in actin cytoskeleton reorganization.

MATERIALS AND METHODS

Cells

Human monocyte–derived DCs were obtained as described (Sallusto and Lanzavecchia, 1994). At day 6, maturation of DCs was induced by LPS (10 ng/ml, Sigma Chemical Co., St. Louis, MO). $CD4^+$ T-cell clone S3085B (S3) were generated as described (Montoya *et al.*, 2002a). PPL-1, a Jurkat cell line variant deficient for ICAM-3 surface expression was provided by F. Lozano (Hospital Clinic I Provincial de Barcelona; Lozano *et al.*, 1993), and PPL-1 stably transfected with ICAM-3 (PPL1-ICAM-3) was generated by J. M. Serrador (Servicio de Inmunología, Hospital de La Princesa, Madrid, Spain). Human $CD4^+$ $CD45RA^+$ $CD45RO^-$ naive Th-cells were isolated from human PBMC using negative selection CD4/CD45RO columns kit (R&D Systems, Minneapolis, MN).

Antibodies and Reagents

We used the following mouse anti-human mAbs: DCIS1/21 (anti-MHC-II; Mittelbrunn *et al.*, 2002), HP2/19 (anti-ICAM-3), Hu5/3 (anti-ICAM-1), TP1/40 (anti-αL integrin chain), D3/9 (anti-CD45), anti-CD14, T3b (anti-CD3), anti-CD81 (I33.22), FN1 (tetraspanin associated anti-MHC-II), 448 (anti-TCR ζ chain or CD247), anti-α tubulin, TS1/11 (blocking anti-αL integrin chain), and HP2/1 (anti-VLA-4). MR1 monoclonal antibody (mAb; anti-DC-SIGN) was from Dr. A. L. Corbí (Centro deInvestigaciones Biológicas, Madrid, Spain), and the blocking anti-DC-SIGN (AZN-D1) was from by Dr. Y. van Kooyk (University Medical Center, Amsterdam, The Netherlands). An additional blocking anti-DC-SIGN mAb was obtained from R&D (clone 120507). Blocking anti-CD11d (240I) was from Dr. D. E. Staunton (ICOS, Bothell, WA). pAb against phosphorylated (Tyr 174) Vav1 was kindly provided by Dr. X. R. Bustelo (CIC, Salamanca, Spain). pAb against total Vav1 was purchased from Upstate Biotechnology (Lake Placid, NY). Antibody against Rac1 was from Transduction Laboratories (Becton Dickinson, Mountain View, CA). ICAM-1-Fc, consisting of the entire extracellular portion of human ICAM-1 fused to human IgG Fc was generated and, ICAM-3-Fc was kindly provided by Dr. M. Robinson (Celltech, Cambridge, UK). Recombinant human fibronectin, poly(L)lysine (PLL), and SEB were from Sigma. Human recombinant IL-2 (Hoffmann-La Roche Nutley, NJ) was from the NIH AIDS Research and Reference Reagent program. CM-TMR (chloromethylbezoylaminotetrametil-Rhodamine) and CMAC (choromethyl derivative of aminocoumarin) fluorescent cell trackers were from Molecular Probes (Eugene, OR). The antagonist of LFA-1,(R)-5 (4-bromobenzyl)-3 (3,5-dichlorophenyl)-1,5-dimethylimidazolidine-2,4-dione (BIRT 377) was kindly provided by T. A. Kelly (Boehringer Ingelheim Pharmaceuticals, Ridgefield, CT). CS3 (control peptide) was kindly provided by Dr. A. García-Pardo (Centro deInvestigaciones Biológicas, Madrid, Spain). D(+) mannose, Latrunculin A (LatA), taxol, and glycophorin were from Sigma.

Conjugate Formation and Immunofluorescence Assays

S3 T-cells were loaded with the blue fluorescent cell tracker CMAC (5 μM for 30 min at 37°C), washed, and resuspended in Hanks' balanced salt solution (HBSS) supplemented with fetal bovine serum 2%. Human mature DC (5×10^4), preloaded with SEB (1 μg/ml for 30 min at 37°C), were mixed with S3 cells (1.5×10^6), centrifuged, and incubated for 15 min at 37°C. Then, cells were allowed to settle on coverslips for 30 min at 37°C. Cellular conjugates using PPL-1, PPL-1-ICAM-3 Jurkat T-cells, or naive T-cells in absence of SEB, were also performed.

Cell conjugates were fixed for 5 min in 4% formaldehyde-phosphate-buffered saline (PBS) and stained with the indicated antibodies, using a goat anti-mouse Alexa 488 highly cross-adsorbed IgG as secondary antibody. For double immunostaining, conjugates were blocked for 1 h with mouse serum and then incubated with a biotinylated anti-ICAM-1 (MEM-111) or an anti ζ chain (448) mAbs, using streptavidin rhodamine red-X or a rabbit anti-mouse Rho-X as secondary reagents, respectively. Clustering of molecules at cell-cell contacts was analyzed by Leica TCS-SP confocal laser scanning unit equipped with Ar and He-Ne laser beams and attached to a Leica DMIRBE inverted epifluorescence microscope or by DMR photomicroscopy using Leica QFISH 1.0 software when indicated (Mannheim, Germany). Cell conjugates forming IS were identified by the presence of a TCR-ζ chain cluster.

Expression of Recombinant DNA Constructs

Chimeric MHC-II-GFP kindly provided by Dr. J. Neefjes (The Netherlands Cancer Institute), CD44-, ICAM-3-, ICAM-1- and αL-GFP were used for dynamic assays. Mature DCs at 7 d (2×10^6 cells) were transiently transfected by nucleoporation with an Amaxa Nucleofector (Amaxa, Cologne, Germany) according to the manufacturer's instructions. After electroporation, DCs were cultured for 16 h on six-well plates in the presence of IL-4 and GM-CSF and then were used for dynamic assays.

Time-lapse Fluorescence Confocal Microscopy

Coverslips were coated with fibronectin (20 μg/ml) for 2 h at 37°C and blocked with PBS containing bovine serum albumin (BSA) 0.1% for 30 min at 37°C. Then, coverslips were washed with HBSS and mounted in Attofluor open chambers (Molecular Probes) and placed on the microscope stage. DCs (8×10^4) preloaded with SEB were allowed to adhere on these chambers for 30 min. CD4 T-cell clone (4×10^5) previously incubated with 5 μg/ml CM-TMR were added to the chambers containing adhered DCs and maintained at 37°C in a 5% CO_2 atmosphere. Confocal images were acquired using Leica TCS-SP confocal laser scanning unit equipped with Ar and He-Ne laser beams and attached to a Leica DMIRBE inverted epi-fluorescence microscope. We used the 63× objective and processed and assembled the images into movies using Leica confocal software.

Ligand-coated Microspheres

Styrene divinilbenzene latex beads (6 μm, Sigma) were coated with ICAM-1-Fc, ICAM-3-Fc, or both as follows. Latex beads were resuspended in adhesion buffer ($NaCO_3$, $NaHCO_3$) and incubated with an anti-human IgG mAb (Fc specific, Sigma), for 2 h at RT. Beads were washed twice and incubated with the Fc-chimerical proteins (10 μg/ml) in 0.4 ml of adhesion buffer overnight at 4°C. After washing with PBS, ligand-coated beads were resuspended in BSA 1% wt/vol and stored at 4°C. The presence of ICAM-1 and ICAM-3 recombinant proteins on microspheres was corroborated by flow cytometry with specific mAbs. For control assays, latex beads were coated with BSA 1%, anti-human IgG mAb (Fc specific), or glycophorin (10 μg/ml, Sigma).

DC-microspheres Conjugates and Cluster Analysis

Immature or mature DC cells (5×10^5) were mixed with latex beads (1×10^6) precoated with ICAM-1 and ICAM-3, incubated for 15 min at 37°C in HBSS 2% BSA, and plated on fibronectin-coated slides. Slides were fixed, immunostained for MHC-II, CD81, CD86, FN1, LFA-1, CD45, or actin and analyzed by confocal microscopy. In some experiments, DC were pretreated with 1 μM latrunculin A or 10 μM Taxol for 20 min at 37°C. When indicated, DCs were preincubated with two blocking anti-DC-SIGN mAbs (AZN-DI and clone 120507), D(+) mannose (100 mM), blocking anti-LFA-1 αL (TS1/11) 10 μg/ml, blocking anti-CD11d (240I) 40 μg/ml, anti-VLA-4 (10 μg/ml), BIRT377 (20 μM), or CS3 (control peptide) for 15 min at 37°C. Clustering of molecules at the contact of DC with latex microspheres was analyzed by Leica TCS-SP confocal laser scanning unit. Clustering was defined as an increment of fluorescence intensity at the contact area compared with the rest of the DC membrane using Leica confocal software.

Determination of Active Vav1 and Rac1

DC (0.5×10^5) were resuspended in RPMI 1640 medium (Flow Laboratories, Irvine, United Kingdom) containing 0.1% BSA and incubated with microspheres coated with ICAM-1-Fc, ICAM-3-Fc, or both. Microspheres coated with anti-Fc or glycophorin were used as controls. After incubation, cells were washed twice with ice-cold HBSS and lysed at 4°C in buffer containing 50 mM Tris, pH 7.4, 100 mM NaCl, 10% glycerol, 1% Nonidet P-40, 2 mM $MgCl_2$, 1 mM phenylmethylsulfonyl fluoride, 2 mM benzamidine, and COMPLETE cocktail inhibitor tablets (Roche Boehringer Mannheim, Indianapolis, IN). The protein content in the cell lysates was measured using protein detection kit (Bio-Rad, Hercules, CA). Samples were separated in 7% SDS-PAGE in the case of Vav and transferred to nitrocellulose membranes. For pulldown experiments GST-PAK-CD, which binds to active Rac, donated by J. Collard (The Netherlands Cancer Institute, Amsterdam, The Netherlands), was prepared as described (Sander *et al.*, 1999). Equal amounts of protein were incubated with glutathione-agarose beads coupled to GST-PAK-CD for 60 min at 4°C and then washed four times in lysis buffer, resuspended in Laemmli buffer, separated in 15% SDS-PAGE, and transferred to nitrocellulose membranes. Western blot was performed using an antibody against Rac1 or phosphorylated (Tyr 174) Vav1, followed by an HRP-conjugated anti-mouse or anti-rabbit serum. For Vav1 total detection nitrocellulose membranes were stripped with Restore Western Blot Stripping buffer (Pierce, Rockford, IL), blocked, and then incubated with anti-Vav. Detection of chemiluminescence was performed using SuperSignal Pico detection kit from Pierce. For statistical purposes, gels of active and total Rac1 or Vav1 were subjected to densitometric analysis and normalized with respect to the loading control. Arbitrary units obtained for incubation point were then referred to the value of cells treated with Fc-coated microspheres to obtain fold induction.

Statistical Analysis

Data obtained were compared by the nonparametrical Mann-Whitney *U*-test with an alpha value of 0.05.

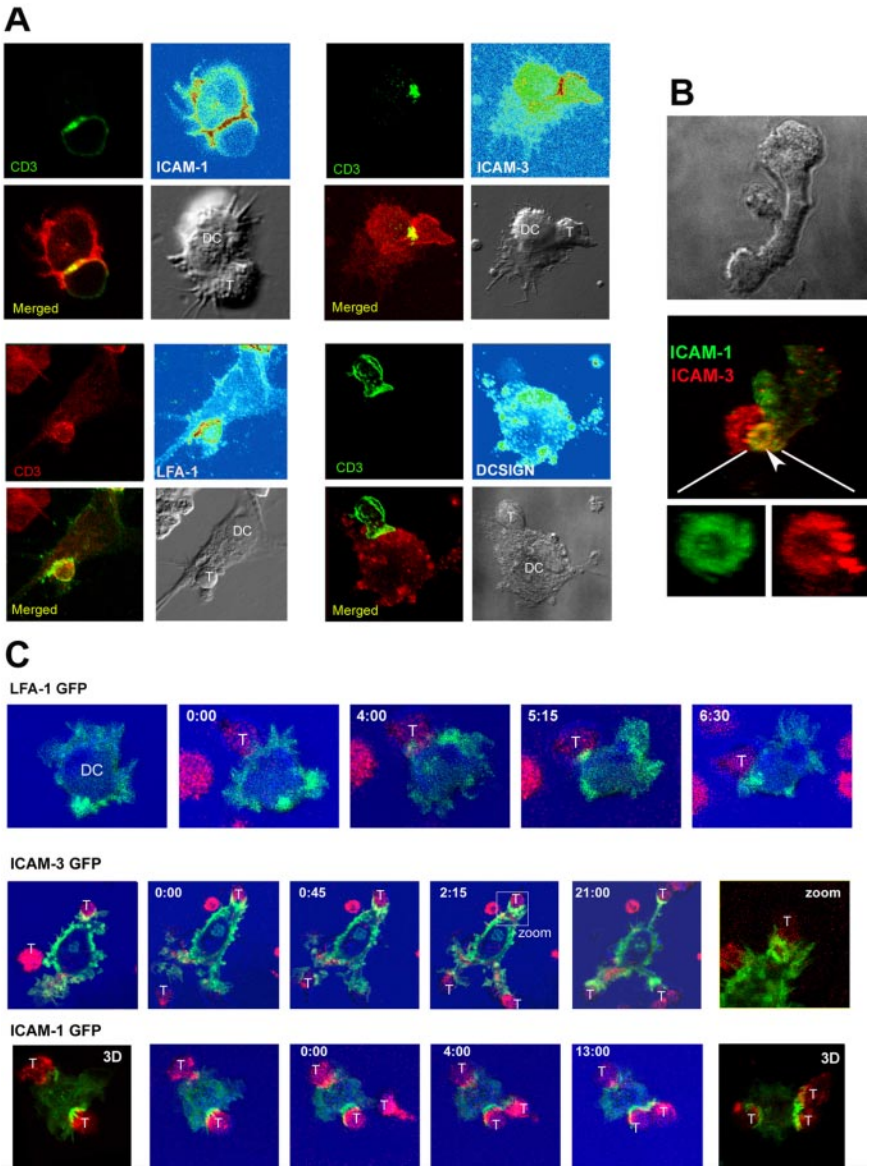

Figure 1. Organization and dynamics of adhesion molecules on DC-T-cell synapses. Human monocyte derived DCs and S3 T-cells were conjugated in the presence of superantigen, stained, and analyzed by confocal microscopy. (A) Representative conjugates stained with CD3/ICAM-1, CD3/ICAM-3, CD3/LFA-1, or CD3/DC-SIGN are shown. Intensity maps correspond at adhesion molecules expression, red indicated maximal fluorescence intensity. DIC and merged images are also shown. (B) ICAM-1 and ICAM-3, at the pSMAC on the contact area. DIC image and 3D reconstruction are shown; arrowhead indicates peripheral adhesion ring; a high magnification of peripheral adhesion ring is also shown. (C) Dynamics of LFA-1, ICAM-3, and ICAM-1 during interaction of DC with T-cells. Mature DCs expressing LFA-1-, ICAM-3-, or ICAM-1-GFP were incubated with SEB and adhered to fibronectin-coated coverslips mounted in chambers. Specific S3 T-cells clone labeled in red with cytoplasmic fluorescent probe CMTMR were added to the chambers, and IS formation was monitored by time-lapse confocal microscopy. Each time point shows the DIC images overlaid with the fluorescence images of the lymphocytes (red) and GFP constructs (green) taken from the digital movie at the times indicated. Time frames were selected based on clear redistribution events. Time 0:00 corresponds to the first contact between cells. Right panels correspond to a high magnification (zoom) of the contact area in the case of ICAM-3-GFP or to a three-dimensional reconstruction (3D) of ICAM-1-GFP last time frame.

RESULTS

Adhesion Molecules in DC-T-cell Synapses

ICAM-3 is essential in the initial scanning of the APC surface by T-cells, clustering at the contact area during the first stages of the T-APC contact (Montoya *et al.*, 2002a). Such clustering at the T-cell side of the IS prompted us to investigate the distribution of their two main counterreceptors, DC-SIGN and LFA-1. First, we studied the localization of LFA-1, ICAM-3, ICAM-1, and DC-SIGN in conjugates formed between SEB specific $CD4^+$ T lymphocytes (S3 T-cells) and SEB-loaded DC (Figure 1A). To recognize mature IS, only those conjugates in which T-cells showed the specific clustering of CD3 or CD3-associated ζ chain were analyzed. ICAM-3, ICAM-1, and LFA-1 were detected at the contact area, forming a clear peripheral ring (Figure 1, A and B). Although DC-SIGN has been described as an important counterreceptor for ICAM-3 (Geijtenbeek *et al.*, 2000), it did not concentrate at the interface of DC-T-cell contacts (Figure 1A). CD11d is another integrin described as counterreceptor for ICAM-3 (Van der Vieren *et al.*, 1995), this molecule is weakly expressed on human monocyte derived-DC and failed to redistribute at the IS (unpublished data).

The dynamic behavior of LFA-1, in addition to that of ICAMs, was studied in primary DC transiently transfected with GFP constructs by time-lapse fluorescence confocal microscopy during DC interactions with SEB-specific T lymphocytes (Figure 1C). LFA-1 redistributed to the contact area; the first clusters were found 4 min after the cellular interaction (Figure 1C and Supplementary Video 1). These clusters were small at the beginning, but evolved into well-organized clusters, which redistributed to the peripheral ring upon conjugate stabilization. Both ICAM-3 and ICAM-1 also redistributed rapidly to the DC contact area with the T lymphocyte (Figure 1C). ICAM-3 was the first molecule that localizes at the DC site of interaction after contact with T lymphocyte. We observed the presence of small transient clusters of ICAM-3 within the first 45 s (Figure 1C). On conjugate stabilization, ICAM-3 was accumulated at the outer zone of the cell-cell contact (zoom Figure 1C). ICAM-1 redistributed later to the contact area (Figure 1C). Like

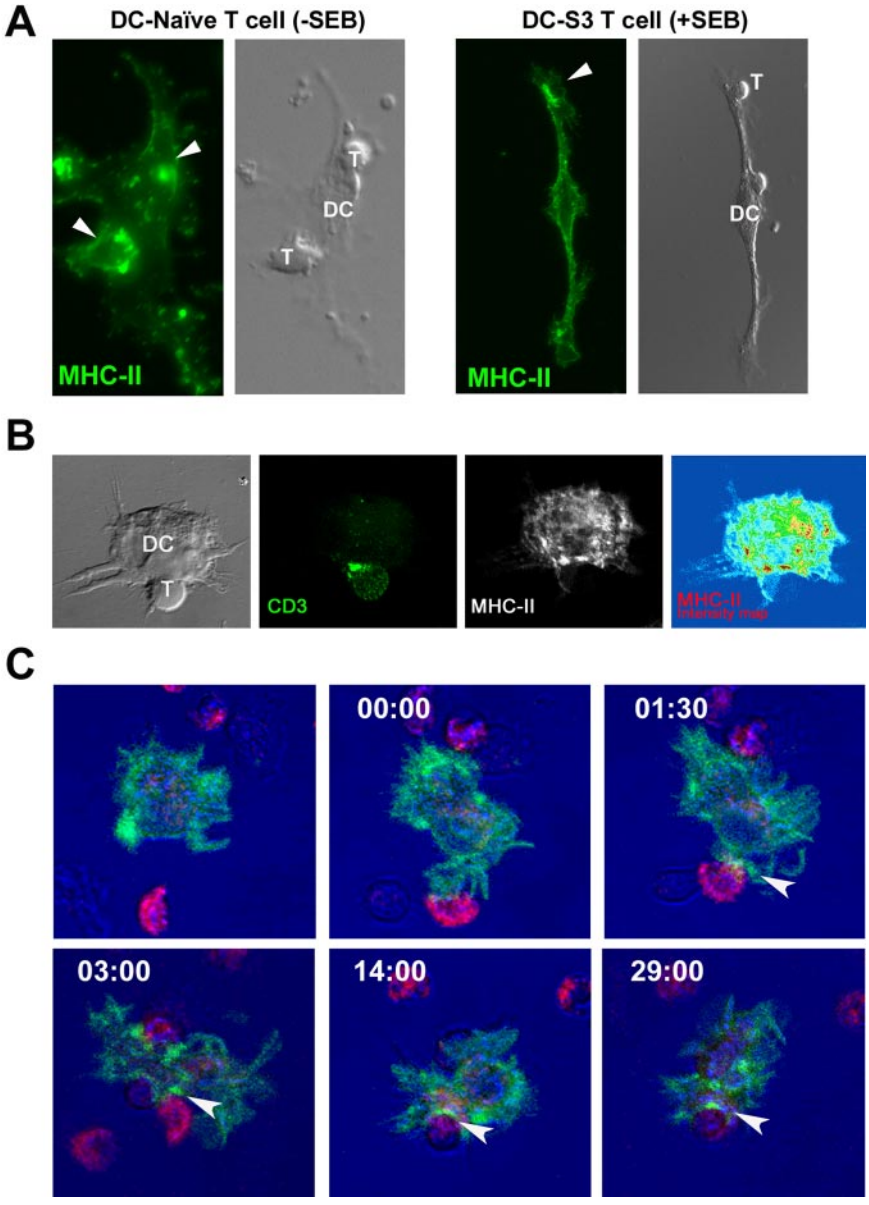

Figure 2. Dynamic redistribution of MHC class II molecules on DC-T-cell interaction. (A) Conjugates of mature DC with naive T-cells (left panel) or S3 T-cells (right panel) in the absence or presence of SEB stained with anti-MHC class II (green). Arrowheads points to the contacts with T-cells. (B) Conjugates of mature DC-S3 T-cell in the presence of SEB were stained with anti-MHC-II DCIS1/21 and anti-CD3 (green). MHC-II expression is shown in both black and white and intensity map images. (C) Dynamics of MHC-II molecules during DC-T-cell interaction. Mature DCs expressing MHC-II-GFP contacting with T-lymphocytes (red) were monitored as in Figure 1. Arrowheads indicate MHC-II-GFP clustering.

ICAM-3, we observed that upon conjugate stabilization ICAM-1 was distributed at the outer zone, forming a peripheral ring. As control, no relocation of CD44 was observed during the process of DC-T-cell conjugate formation (Supplementary Video 2).

Early MHC-II Clustering on DC-T-cell Conjugates

MHC-II localization at DC-T-cell conjugates was analyzed. The presence of MHC-II on DC at the contact area was observed in conjugates with either peripheral blood naïve T-cells with DC in the absence of antigen or S3 T-cells with DC pulsed with SEB (Figure 2A). Confocal microscopy studies showed the colocalization of clusters of MHC-II molecules on DC with CD3 at T-cell side (Figure 2B). Dynamic videomicroscopy assays revealed the unexpected finding of a rapid clustering of MHC class II molecules at the contact area, forming discrete transient clusters 1.5 min after conjugate formation, which were more evident 12–30 min later and suggest a possible role for this molecule during the first stages of synapse formation (Figure 2C and Supplementary Video 3).

ICAMs Trigger MHC-II Clustering in DC

To investigate whether LFA-1 engagement influences MHC class II redistribution on membrane DC, we studied the reorganization of LFA-1 and MHC-II in DCs upon conjugation with latex microspheres coated with human recombinant ICAM-1-Fc, ICAM-3-Fc, or both. LFA-1 clustering was markedly enhanced at the area of cell contact with ICAM-1-latex microspheres, whereas ICAM-3 induced a lower clustering. Interestingly, ICAM-3-microspheres binding, induced formation of MHC-II clusters at the contact area with DC in a large percent of conjugates (Figure 3A). In contrast with LFA-1 clustering, ICAM-3 tended to be a more efficient inductor of MHC-II clustering than ICAM-1. We also found that microspheres coated with both ICAM-1 and ICAM-3 exerted an additive effect on MHC-II relocation (Figure 3A). The fluorescence intensity of MHC-II in the contact area

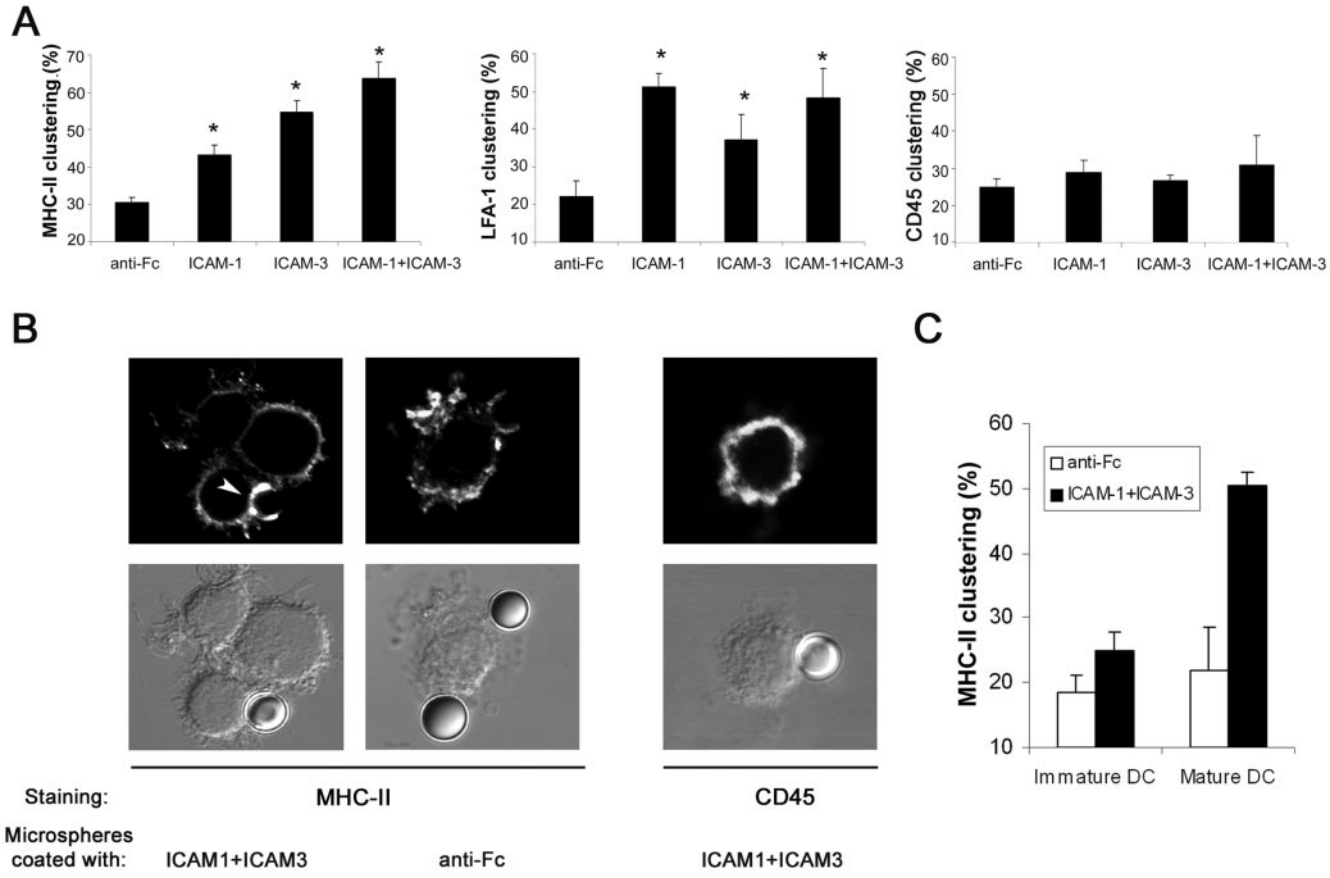

Figure 3. ICAM-3 induces the clustering of MHC-II molecules on DC. (A) Clustering of LFA-1, MHC-II, and CD45 induced by ICAM-1 and ICAM-3. Mature DCs were mixed with latex microspheres coated with recombinant human ICAM-1-, ICAM-3-Fc, or both. Latex microspheres coated with anti-Fc were used as controls. Conjugates were stained with anti-LFA-1, anti-MHC-II, or anti-CD45 and analyzed for redistribution of these molecules by confocal microscopy. Thirty DCs-microspheres latex beads conjugates were counted in each experiment. Results are expressed as percent of DCs showing molecular relocation. Data represent mean ± SEM of four independent experiments. (B) Distribution of MHC-II and CD45 in conjugates between DC and ICAM-1+ICAM-3– and anti-Fc–coated microspheres. Image corresponds to one confocal section. Arrowhead shows molecular clustering. (C) MHC-class II clustering is specific of mature DCs. Immature or mature DCs were conjugated with ICAM-1+ICAM-3–Fc coated microspheres, and relocation of MHC-class II was determined.

with ICAMs was twofold higher than the rest of the DC membrane fluorescence (Table 1). This phenomenon was specific of MHC-II since the leukocyte-specific molecule CD45 was not clustered under the same experimental conditions (Figure 3, A and B, and Table 1).

Interestingly, clustering of MHC class II molecules at the contact area seems to be intrinsic to mature DC, whereas immature DCs and other APCs analyzed such as Raji and LG-2 B cells were unable to redistribute MHC-II in the presence of ICAM-coated latex microspheres (Figure 3C, and unpublished data).

DC-SIGN and CD11d are other counterreceptors for ICAM-3 besides LFA-1 (Geijtenbeek *et al.*, 2000). To assess the role of these molecules in MHC-II clustering, DCs were incubated with blocking reagents against LFA-1, DC-SIGN, and CD11d before the addition of ICAMs latex microspheres. BIRT 377 (Kelly *et al.*, 1999; Woska *et al.*, 2003), and the blocking anti-αL chain mAb (TS1/11), were used to impair function of LFA-1; D(+) mannose, and two mAb (AZN-DI and clone 120507) were used to block DC-SIGN and blocking anti-CD11d (240I) to inhibit CD11d. Anti-VLA-4 mAb was used as control. BIRT 377 prevented clus-

Table 1. Quantification of fluorescence intensity at the contact area between DCs and ICAMs-coated latex microspheres[a]

	ICAM-1+ICAM-3		Anti-Fc	
Staining	Contact area	DC membrane	Contact area	DC membrane
MHC-II	179.5 ± 30.6[b]	86.5 ± 43.8	96.7 ± 25.4	90.5 ± 28
CD45	160.4 ± 40.02	158.8 ± 34.2	152.7 ± 30.6	157.8 ± 33.6

Mean arithmetic ± SD are shown, n = 10, [b]$p < 0.05$.

[a] Data correspond to mean fluorescence intensity.

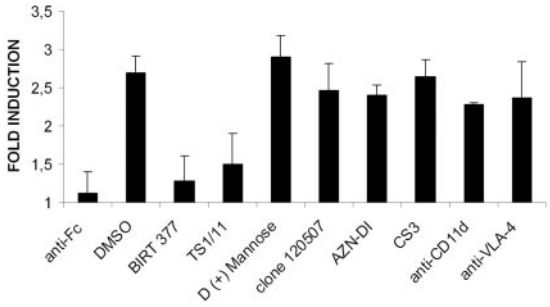

Figure 4. MHC-II relocation induced by ICAMs is LFA-1 dependent. Relocation of MHC-II molecules at the contact area between DC and ICAM-coated microspheres was analyzed in the presence of two different anti-DC-SIGN–blocking antibodies (AZN-DI and clone 120507, 10 μg/ml), D (+) mannose (100 mM), BIRT 377 (20 μM), anti-aL TS1/11(10 μg/ml), anti-CD11d 240I (40 μg/ml), CS3 (control peptide), or anti-VLA-4 (10 μg/ml) as isotype control. Bars represent the fold induction of MHC-II relocation induced by ICAMs relative to that induced by glycophorin-coated latex microspheres of three independent experiments. *$p < 0.05$.

tering of LFA-1 induced by ICAM-1 or ICAM-1 + ICAM-3 (unpublished data). Remarkably, clustering of MHC-II induced by ICAM-3 or ICAM-1 + ICAM-3 was also significantly reduced by LFA-1 blockade (BIRT 377 and mAb TS1/11), whereas no effect was observed with inhibitors of DC-SIGN, CD11d, or VLA-4 (Figure 4 and unpublished data). These results point to LFA-1 as the major DC counterreceptor for ICAM-3 and ICAM-1 involved in MHC-II clustering.

The local density of MHC-II molecules loaded with Ag peptides, along with the presence of costimulatory molecules determine the avidity of APC-T-cell interactions (Reay *et al.*, 2000). It has been described that a subset of di- or oligomerized MHC-II molecules localizes to tetraspanin-based microdomains (Kropshofer *et al.*, 2001). We have found that ICAM-3 is also able to induce the clustering of CD81 (unpublished data), a member of tetraspanin family. Moreover, we have detected MHC class II clustering using the FN1 mAb (unpublished data), which specifically recognize tetraspanin-associated MHC-II molecules (Drbal *et al.*, 1999).

To further confirm the role of ICAM-3 in MHC-II clustering, DC-T-cell conjugates were formed either with ICAM-3–deficient PPL1 T-cells or with PPL-1 cells stably transfected with ICAM-3 (PPL1-ICAM-3). Both PPL1 and PPL1-ICAM-3 displayed comparable levels of ICAM-1 (Figure 5A). MHC-II clustering was detected in a large percent of DCs in conjugates with PPL1-ICAM-3 compared with a lower proportion of PPL1 cells (Figure 5, B and C; 58.13% ± 9.9 vs. 24.8% ± 6.7). In addition, DCs in conjugates with PPL1-ICAM-3 cells also showed a clear relocation of the costimulatory molecule CD86 to the contact area (Figure 5, B and C), which postulates a role for ICAMs not only in MHC-II clustering but in relocation of costimulatory molecules for efficient Ag pre-

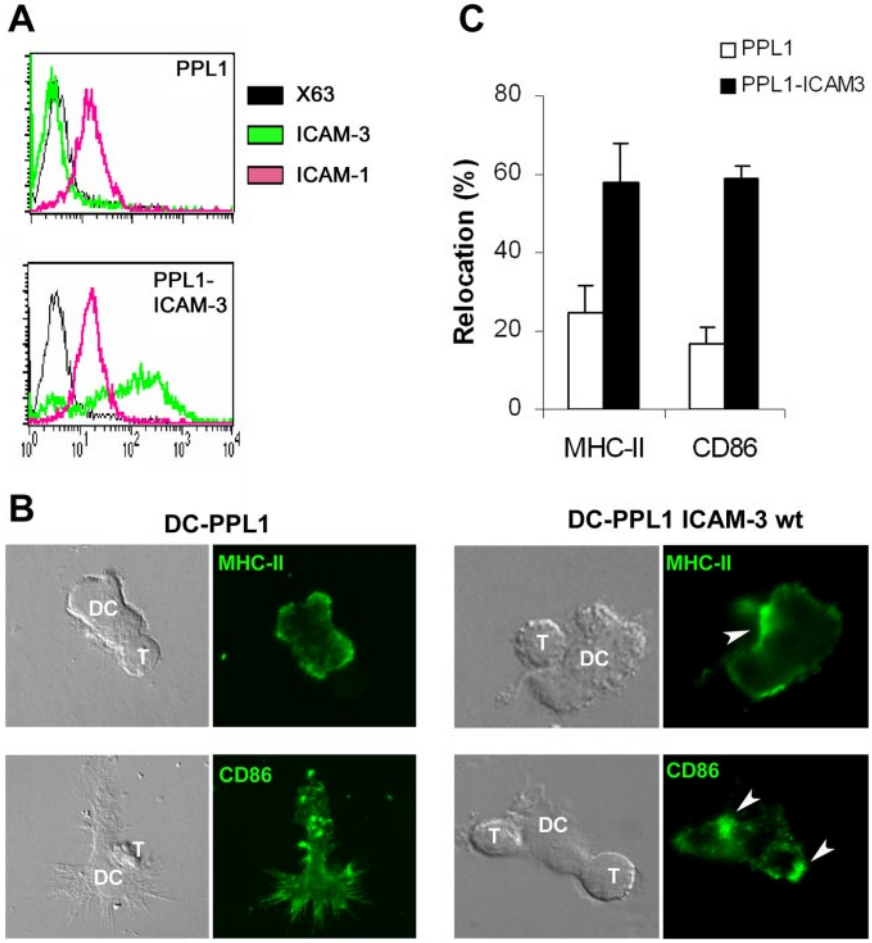

Figure 5. ICAM-3 induces clustering of MHC-II and CD86 to DC-T-cell synapses. (A) Flow cytometry analysis of ICAM-1 and ICAM-3 expression on PPL-1 cells. (B) MHC-II and CD86 on DC conjugates with PPL1 or PPL1-ICAM-3. (C) Mature DCs were mixed with PPL-1 (Jurkat T-cells ICAM-3 negative) or PPL-1 stably transfected with ICAM-3. Conjugates were fixed and stained with anti-MHC-II or anti-CD86. Data are mean ± SEM of three independent experiments. Bars represent the mean relocation of MHC-II or CD86 relative to number of DC-PPL-1 conjugates. Arrowheads show molecular clustering at DC-PPL-1 contact.

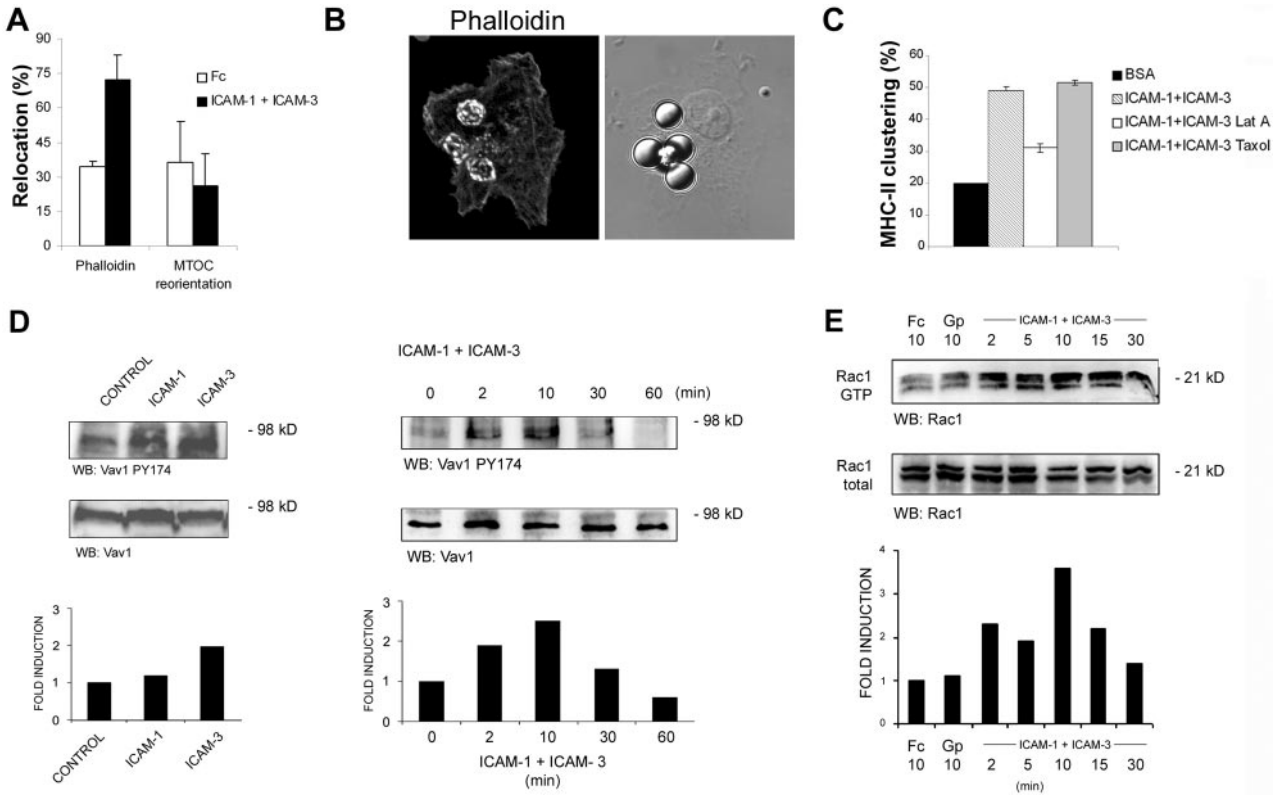

Figure 6. Actin cytoskeleton reorganization and activation is involved on MHC-II clustering mediated by ICAMs. (A) Clustering of actin and tubulin cytoskeleton on conjugates between DC and ICAM-1+ICAM-3–coated microspheres. (B) Actin polarization on DC induced by ICAMs. Orthogonal projection of confocal image of a representative conjugate between DC and ICAM-1+ICAM-3-microspheres stained with phalloidin is shown. (C) MHC-II relocation on conjugates between DC and ICAM-1+ICAM-3 microspheres generated in presence of actin (latrunculin A) and tubulin (taxol) inhibitors. (D) ICAMs induce Vav1 phosphorylation in DC. Cells were incubated with ICAM-1, ICAM-3, ICAM-1+ICAM-3, or anti-Fc–coated microspheres for indicated times, and the level of phosphorylation of Tyr174 (PY174) was assessed by Western blot. A representative experiment out of four performed is shown. (E) ICAMs induce activation of Rac1 in DC. Cells were stimulated as in D and pulldown experiments were performed using GST-PAK-CD as bait. Western blot on pulldown and total lysate fractions were carried out. A representative experiment out of four performed is shown.

sentation. Thus, ICAM-3 binding to LFA-1 on DC rearranges the Ag presentation and costimulatory molecular machinery at the DC interface with the T-cell.

Actin Cytoskeleton on MHC-II Clustering Induced by ICAMs

The actin cytoskeleton is critical for the assembly of signaling components and the formation of the IS (Dustin and Cooper, 2000). We found that ICAM-3 and ICAM-1 were able to induce actin reorganization at the contact area of DC with ICAM-3+ICAM-1–coated latex microspheres. Our results show not only that ICAMs binding triggers actin rearrangement on the interacting area of DC (Figure 6, A and B), but also that the disruption of actin cytoskeleton impairs MHC-II clustering. In this regard, clustering of MHC-II induced by ICAM-3 was blocked by Latrunculin A, an inhibitor of actin polymerization, but no significant effect was exerted by tubulin disrupting drugs such as taxol (Figure 6C). These data support the active role of the DC actin cytoskeleton during IS formation. In contrast, DC microtubular network and MTOC positioning remain unaffected by ICAM-mediated initial cellular interactions (Figure 6A).

To assess whether the actin cytoskeleton-associated signaling machinery is triggered by ICAMs engagement on DC, we analyzed the activation of Vav1 and GTPase Rac, two key molecules in actin cytoskeleton rearrangement. Phosphorylation of Vav1 in Tyr 174, which is essential for Vav1 activation, was studied in DC stimulated with latex microspheres coated with ICAM-1, ICAM-3, or both. ICAM-3, and ICAM-1 to a lower extent, induced Vav1 phosphorylation at this residue with a kinetics profile that peaked at 10 min (Figure 6D). Consistent with Vav1 activation, Rac1 activation was also observed in DC treated with ICAMs (Figure 6E). The kinetics of Rac1 activation correlated with that of Vav1 phosphorylation, suggesting that the activation of Vav1 and Rac1 are causally related (Figure 6E).

DISCUSSION

Until now, most efforts to explore the regulation of the IS have been aimed to T-cells. Furthermore, most studies performed with B-cells as APCs have assigned a passive role to the APC in IS formation. Although DCs are the most important APCs in vivo, relatively little is known on the nature of their IS with T lymphocytes. Here, we describe the localization and dynamics of cell surface molecules involved in IS formation using human monocyte-derived DCs and a $CD4^+$ T-cell clone specific for SEB. Dynamic videomicroscopy assays revealed the unexpected finding of a rapid clustering of MHC class II molecules at the contact area and suggest a

possible role for this molecule during the first stages of synapse formation.

During initial contacts, low-affinity adhesive interactions facilitate the exploration of the DCs surface by T-cells. ICAM-3 is expressed by all leukocytes, particularly by naive T lymphocytes, and is essential in the initial scanning of the APC surface by T-cells, clustering at the contact area during the first stages of the T-APC contact (Montoya *et al.*, 2002a). Interestingly, ICAM-3 binding to LFA-1 on DCs induces the redistribution of MHC-II, which suggests the existence of an adhesion-dependent component in MHC-II lateral mobility on the membrane of the DC. Thus, our data support a key role for ICAM-3 and, to a lower extent ICAM-1, in the initial contact with DCs, mediating cell adhesion and facilitating the priming of T-cells by inducing an enhancement of the density of MHC-II and the costimulatory molecule CD86 on DC-T-cell contact area prior to TCR Ag recognition. These data are further supported by the relocation on DC of MHC class II at the contact area with naïve T-cells in the absence of Ag. Previously it has been described that immunological synapses are formed between DCs and polyclonal naive T-cells in the absence of antigen (Revy *et al.*, 2001). The clustering of MHC class II induced by ICAMs is observed in mature but not immature DCs. In this regard, recent findings have described the presence of organized IS in conjugate of mature, but not immature, DCs with naive T lymphocytes (Benvenuti *et al.*, 2004b).

Our data based on the use of both peptide and antibody blocking reagents demonstrate that LFA-1 is the ICAM-3 counterreceptor implicated in the induction of MHC class II clustering on DCs. It has been previously described that some B lymphoma APC supported CD4 clustering in the absence of antigen or during presentation of null peptides, and this CD4 recruitment was dependent on MHC class II, and LFA-1 on the APC (Zal *et al.*, 2002). LFA-1 is relocalized to the contact area within the first 5 min during the process of IS formation, later than MHC-II molecules. This suggests that an organized cluster of LFA-1 is not required for its role in MHC class II clustering. Also, the apparent temporal dissociation between clustering of MHC-II and of LFA-1 would rule out the simplest explanation of the findings, i.e., that a cluster of MHC-II is induced by ICAM-3 through a lateral association with LFA-1.

ICAM-3–mediated MHC-II clustering may be related to the inclusion of the latter into lipid (rafts) or protein (tetraspanin-based) membrane microdomains (Anderson *et al.*, 2000; Kropshofer *et al.*, 2001; Hemler, 2003). We found that MHC-II molecules clustered by interaction with ICAM-coated microspheres were associated with tetraspanins as demonstrated by CD81 clustering and detection of MHC-II clusters with the mAb FN1. Although it has been reported that MHC-II molecules on B-cells seem to cluster into detergent-resistant membrane microdomains (Anderson *et al.*, 2000), recent evidence indicates that rafts exhibit a random distribution on the T-cell during IS formation (Glebov and Nichols, 2004).

The enrichment of MHC-II at the synapse could be due at least in part to an enhanced polarized transport of intracellular MHC class II to the synapse. In this regard, it has been described that cytochalasin D treatment leads to a delayed appearance of stable forms of class II molecules and a reduced presentation efficiency of Ag determinant in B-cells (Barois *et al.*, 1998). Boes *et al.* (2002) have observed that interaction of Ag-loaded DCs with Ag-specific CD4 T-cells induces the formation of long tubular class II MHC-positive compartments that polarize toward the interacting T-cell. Under our experimental conditions we did not observe those class II MHC compartments. These apparent discrepancies could be attributed to specific characteristics of T-cells and APCs used in the different experimental systems. Thus, in our work, DCs were loaded with SEB, which does not require endosomal processing, and it has been described that endosomal tubulation requires acquisition of peptide in endosomal compartments (Bertho *et al.*, 2003). Our results show not only that ICAM-3 binding triggers actin rearrangement on the interacting area of DC, but also that the disruption of actin cytoskeleton impairs MHC-II clustering. These data that support the active role of the DC cytoskeleton during IS formation complement those previously described by other group (Al-Alwan *et al.*, 2001, 2003) Our data clearly demonstrate that cytoskeletal reorganization is required for ICAM-driven MHC-II clustering.

ICAMs binding to DC triggers activation of Vav1 and GTPase Rac1, in accordance with the promotion of actin rearrangement. Vav1 regulates integrin clustering on the T-cell during Ag presentation (Krawczyk *et al.*, 2002), being involved in TCR-β2 integrin cross-talk during this process (Ardouin *et al.*, 2003). Despite being expressed on DC and B-cells, the role of Vav in supramolecular activation on the APC side of the IS has not yet been addressed. Recently, it has been described the role of both Rac1 and Rac2 in the initial phases of DC-T-cell interactions and in T-cell priming. Rac1/2$^{-/-}$ DCs have an impaired ability to interact with naïve T-cells, as well as in priming T-cells (Benvenuti *et al.*, 2004a). Our data provide a mechanism to Rac activation in DCs by naïve T-cells at early phases of synapse formation, linking cytoskeletal rearrangements with clustering of plasma receptors such as LFA-1 and MHC-II molecules to the DC area in close contact with T-cells.

In summary, our results demonstrate that the initial binding mediated by ICAM-3 at the T-cell side, to LFA-1 on the DC side triggers the clustering of MHC class II and other costimulatory molecules toward DC synapse area, before Ag recognition by TCR. This provides a mechanism for a more efficacious presentation of peptide-MHC complexes by DCs.

ACKNOWLEDGMENTS

We are grateful to Dr. R. Gonzalez Amaro and Dr. A. L. Corbí for the critical reading of this manuscript. This work was supported by grants BMC02-00536 and Ayuda a la Investigación Básica Juan March 2002 to F. Sánchez-Madrid. M.M. is supported by FPU AP2000-0279 from the Ministerio deEducación, Cultura y Deporte.

REFERENCES

Al-Alwan, M., Rowden, G., Lee, T., and West, K. (2001). The dendritic cell cytoskeleton is critical for the formation of the immunological synapse. J. Immunol. *166*, 1452–1456.

Al-Alwan, M. M., Liwski, R. S., Haeryfar, S. M., Baldridge, W. H., Hoskin, D. W., Rowden, G., and West, K. A. (2003). Cutting edge: dendritic cell actin cytoskeletal polarization during immunological synapse formation is highly antigen-dependent. J. Immunol. *171*, 4479–4483.

Anderson, H. A., Hiltbold, E. M., and Roche, P. A. (2000). Concentration of MHC class II molecules in lipid rafts facilitates antigen presentation. Nat. Immunol. *1*, 156–162.

Ardouin, L., Bracke, M., Mathiot, A., Pagakis, S. N., Norton, T., Hogg, N., and Tybulewicz, V. L. (2003). Vav1 transduces TCR signals required for LFA-1 function and cell polarization at the immunological synapse. Eur. J. Immunol. *33*, 790–797.

Banchereau, J., and Steinman, R. M. (1998). Dendritic cells and the control of immunity. Nature *392*, 245–252.

Barois, N., Forquet, F., and Davoust, J. (1998). Actin microfilaments control the MHC class II antigen presentation pathway in B cells. J. Cell Sci. *111*, 1791–1800.

Benvenuti, F., Hugues, S., Walmsley, M., Ruf, S., Fetler, L., Popoff, M., Tybulewicz, V. L., and Amigorena, S. (2004a). Requirement of Rac1 and Rac2 expression by mature dendritic cells for T cell priming. Science *305*, 1150–1153.

Benvenuti, F., Lagaudriere-Gesbert, C., Grandjean, I., Jancic, C., Hivroz, C., Trautmann, A., Lantz, O., and Amigorena, S. (2004b). Dendritic cell maturation controls adhesion, synapse formation, and the duration of the interactions with naive T lymphocytes. J. Immunol. *172*, 292–301.

Bertho, N., Cerny, J., Kim, Y. M., Fiebiger, E., Ploegh, H., and Boes, M. (2003). Requirements for T cell-polarized tubulation of class II+ compartments in dendritic cells. J. Immunol. *171*, 5689–5696.

Bleijs, D., Binnerts, M. E., van Vliet, S. J., Figdor, C. G., and van Kooyk, Y. (2000). Low-affinity LFA-1/ICAM-3 interactions augment LFA-1/ICAM-1-mediated T cell adhesion and signaling by redistribution of LFA-1. J. Cell Sci. *113*, 391–400.

Boes, M., Cerny, J., Massol, R., Op den Brouw, M., Kirchhausen, T., Chen, J., and Ploegh, H. L. (2002). T-cell engagement of dendritic cells rapidly rearranges MHC class II transport. Nature *418*, 983–988.

Campanero, M. R., del Pozo, M. A., Arroyo, A., Sanchez-Mateos, P., Hernandez-Caselles, T., Craig, A., Pulido, R., and Sanchez-Madrid, F. (1993). ICAM-3 interacts with LFA-1 and regulates the LFA-1/ICAM-1 cell adhesion pathway. J. Cell Biol. *123*, 1007–1016.

Drbal, K., Angelisova, P., Rasmussen, A. M., Hilgert, I., Funderud, S., and Horejsi, V. (1999). The nature of the subset of MHC class II molecules carrying the CDw78 epitopes. Int. Immunol. *11*, 491–498.

Dustin, M. L., and Cooper, J. A. (2000). The immunological synapse and the actin cytoskeleton: molecular hardware for T cell signaling. Nat. Immunol. *1*, 23–29.

Geijtenbeek, T. B., Torensma, R., van Vliet, S. J., van Duijnhoven, G. C., Adema, G. J., van Kooyk, Y., and Figdor, C. G. (2000). Identification of DC-SIGN, a novel dendritic cell-specific ICAM-3 receptor that supports primary immune responses. Cell *100*, 575–585.

Glebov, O. O., and Nichols, B. J. (2004). Lipid raft proteins have a random distribution during localized activation of the T-cell receptor. Nat. Cell Biol. *6*, 238–243.

Grakoui, A., Bromley, S. K., Sumen, C., Davis, M. M., Shaw, A. S., Allen, P. M., and Dustin, M. L. (1999). The immunological synapse: a molecular machine controlling T cell activation. Science *285*, 221–227.

Hemler, M. E. (2003). Tetraspanin proteins mediate cellular penetration, invasion, and fusion events and define a novel type of membrane microdomain. Annu. Rev. Cell Dev. Biol. *19*, 397–422.

Juan, M., Vinas, O., Pino-Otin, M. R., Places, L., Martinez-Caceres, E., Barcelo, J. J., Miralles, A., Vilella, R., de la Fuente, M. A., and Vives, J. (1994). CD50 (intercellular adhesion molecule 3) stimulation induces calcium mobilization and tyrosine phosphorylation through p59fyn and p56lck in Jurkat T cell line. J. Exp. Med. *179*, 1747–1756.

Kelly, T., Jeanfavre, D. D., McNeil, D. W., Woska, J. J., Reilly, P. L., Mainolfi, E. A., Kishimoto, K. M., Nabozny, G. H., Zinter, R., Bormann, B. J., and Rothlein, R. (1999). Cutting edge: a small molecule antagonist of LFA-1-mediated cell adhesion. J. Immunol. *163*, 5173–5177.

Krawczyk, C., Oliveira-dos-Santos, A., Sasaki, T., Griffiths, E., Ohashi, P. S., Snapper, S., Alt, F., and Penninger, J. M. (2002). Vav1 controls integrin clustering and MHC/peptide-specific cell adhesion to antigen-presenting cells. Immunity *16*, 331–343.

Kropshofer, H., Spindeldreher, S., Rohn, T., Platania, N., Grygar, C., Daniel, N., Wolpl, A., Langen, H., Horejsi, V., and Vogt, A. B. (2001). Tetraspan microdomains distinct from lipid rafts enrich select peptide-MHC class II complexes. Nat. Immunol. *3*, 61–68.

Lozano, F., Places, L., Alberola-Ila, J., Mila, M., Villamor, N., Barcelo, J.V.F., and Vives, J. (1993). Isolation and characterisation of a CDw50 negative Jurkat T-cell line variant (PPL. 1). Leuk. Res. *17*, 9–16.

Mittelbrunn, M., Yanez-Mo, M., Sancho, D., Ursa, A., and Sanchez-Madrid, F. (2002). Cutting edge: dynamic redistribution of tetraspanin CD81 at the central zone of the immune synapse in both T lymphocytes and APC. J. Immunol. *169*, 6691–6695.

Monks, C., Freiberg, B., Kupfer, H., Sciaky, N., and Kupfer, A. (1998). Three-dimensional segregation of supramolecular activation clusters in T cells. Nature *395*, 82–86.

Montoya, M., Sancho, D., Bonello, G., Collette, Y., Langlet, C., He, H., Aparicio, P., Alcover, A., Olive, D., and Sanchez-Madrid, F. (2002a). Role of ICAM-3 in the initial interaction of T lymphocytes and APCs. Nat. Immunol. *3*, 159–168.

Montoya, M., Sancho, D., Vicente-Manzanares, M., and Sanchez-Madrid, F. (2002b). Cell adhesion and polarity during immune interactions. Immunol. Rev. *186*, 68–82.

Ostermann, G., Weber, K. S., Zernecke, A., Schroder, A., and Weber, C. (2002). JAM-1 is a ligand of the beta(2) integrin LFA-1 involved in transendothelial migration of leukocytes. Nat. Immunol. *3*, 151–158.

Reay, P., Matsui, K., Haase, K., Wulfing, C., Chien, Y., and Davis, M. (2000). Determination of the relationship between T cell responsiveness and the number of MHC-peptide complexes using specific monoclonal antibodies. J. Immunol. *164*, 5626–5634.

Revy, P., Sospedra, M., Barbour, B., and Trautmann, A. (2001). Functional antigen-independent synapses formed between T cells and dendritic cells. Nat. Immunol. *2*, 925–931.

Sallusto, F., and Lanzavecchia, A. (1994). Efficient presentation of soluble antigen by cultured human dendritic cells is maintained by granulocyte/macrophage colony-stimulating factor plus interleukin 4 and downregulated by tumor necrosis factor alpha. J. Exp. Med. *179*, 1109–1118.

Sander, E. E., ten Klooster, J. P., van Delft, S., van der Kammen, R. A., and Collard, J. G. (1999). Rac downregulates Rho activity: reciprocal balance between both GTPases determines cellular morphology and migratory behavior. J. Cell Biol. *147*, 1009–1022.

Starling, G. C., McLellan, A. D., Egner, W., Sorg, R. V., Fawcett, J., Simmons, D. L., and Hart, D. N. (1995). Intercellular adhesion molecule-3 is the predominant co-stimulatory ligand for leukocyte function antigen-1 on human blood dendritic cells. Eur. J. Immunol. *25*, 2528–2532.

Van der Vieren, M., Le Trong, H., Wood, C., Moore, P. F., St John, T., Staunton, D. E., and Gallatin, W. M. (1995). A novel leukointegrin, alpha d beta 2, binds preferentially to ICAM-3. Immunity *3*, 683–690.

Van Seventer, G. A., Shimizu, Y., Horgan, K. J., and Shaw, S. (1990). The LFA-1 ligand ICAM-1 provides an important costimulatory signal for T cell receptor-mediated activation of resting T cells. J. Immunol. *144*, 4579–4586.

Woska, J. J. *et al.* (2003). Small molecule LFA-1 antagonists compete with an anti-LFA-1 mAb for binding to the CD11a I domain: development of a flow-cytometry-based receptor occupancy assay. J. Immunol. Methods *277*, 101–115.

Zal, T., Zal, M. A., and Gascoigne, N. R. (2002). Inhibition of T cell receptor-coreceptor interactions by antagonist ligands visualized by live FRET imaging of the T-hybridoma immunological synapse. Immunity *16*, 521–534.